Lattice dynamics and inelastic neutron scattering studies of MFX (M=Ba, Sr, Pb; X=Cl, Br, I)

R. Mittal,[1] S. L. Chaplot,[1] A. Sen,[1] S. N. Achary,[2] and A. K. Tyagi[2]
[1]*Solid State Physics Division, Bhabha Atomic Research Centre, Trombay, Mumbai 400 085, India*
[2]*Applied Chemistry Division, Bhabha Atomic Research Centre, Trombay, Mumbai 400 085, India*
(Received 20 May 2002; revised manuscript received 13 January 2003; published 15 April 2003)

We report lattice dynamical calculation of technologically important matlockite structured compounds MFX [M(Ba, Sr, Pb); X(Cl, Br, I)] using a transferable interatomic potential based on a shell model. Our model is validated by the inelastic neutron scattering measurement of the phonon density of states for BaFCl carried out using the triple axis spectrometer at Trombay. We have further exploited this model for the calculation of high-pressure and high-temperature thermodynamic properties of these compounds which are found to be in good agreement with various experimental data, as available in the literature. The calculations provide a theoretical understanding of the elastic constants, equation of state, phonon dispersion relations and density of states, thermal expansion, specific heat, Debye temperature, and anisotropic thermal parameters of these materials.

DOI: 10.1103/PhysRevB.67.134303 PACS number(s): 63.20.Dj, 78.70.Nx, 64.30.+t

I. INTRODUCTION

Alkaline earth fluorohalides MFX (M=Ba, Sr, Pb; X=Cl, Br, I) are quite important for their heterogeneous applications in industries. These compounds find utility, for instance, in x-ray image storage properties[1] on dilute doping with rare earth ions and also, as pressure calibrants[2] in diamond anvil cells. Some crystals of such mixed dihalides, viz. BaFCl and BaFBr, are also used, in spectroscopic and nuclear detectors. Further, these compounds are of considerable scientific interest[3–22] due to their layered structure. The crystal structures of these compounds at high pressures have already been studied,[3–6] where the anisotropic behavior of unit cell parameters upon compression is attributed to the anisotropic coordination of the highly polarized halogen ions. High-temperature x-ray diffraction studies have also been reported for BaFCl using single crystal[7] and polycrystalline samples[8] up to about 900 K. Ultrasonic pulse echo and Brillouin scattering techniques[10,11] were used for the measurement of the elastic constants. Measurements of long wavelength Raman and infrared active phonons have been reported[14–17] as well. The specific heat measurements for these compounds were reported[12,13] only in the low temperature region. Further, the structural and electronic properties of alkaline-earth flurohalides at high pressure have been theoretically investigated[19] using the tight-binding linear muffin-tin orbital method. Atomistic simulations have been performed[9,18,22] for the sake of studying the high pressure phase transitions, thermal expansion, and, also, defect properties.

Lattice dynamical calculations have also been reported[20,21] for BaFCl and SrFCl using a shell model involving adjustable force constant parameters at ambient pressure. However, these models, based on force constants, are not transferable to other compounds, and cannot be used for the calculation of theromodynamic properties at high pressures. Further, there are no neutron inelastic scattering data available for this family of compound. Therefore, for a basic understanding of the thermodynamic properties of these compounds we have undertaken a detailed lattice dynamical study of the mixed halide system MFX (M=Ba, Sr, Pb; X=Cl, Br, I) using a shell model with transferable interatomic potentials. The knowledge of their thermodynamic properties would be useful in designing improved materials. In this paper we also report on a measurement of the phonon density of states for BaFCl using the neutron inelastic scattering technique at Trombay. With the transferable shell model, we have been able to calculate the crystal structure, elastic constants, phonon dispersion relations and density of states, equation of state, specific heat, thermal expansion and anisotropic thermal parameters of BaFCl, BaFBr, BaFI, SrFCl, SrFBr, PbFCl and PbFBr. The calculations are found to be in good agreement with the available experimental data.

Section II gives an outline of the experimental technique, as adopted here. Our lattice dynamics calculations are given in Sec. III, followed by the results and discussion, and conclusions in Secs. IV and V, respectively.

II. EXPERIMENT

The starting material BaF_2 is prepared by treating $BaCO_3$ with 40% aqueous hydrofluoric acid. The solution was evaporated to dryness on a hot water bath and then, dried up at 800 °C in a flowing argon atmosphere. $BaCl_2$ was subsequently prepared by dehydrating $BaCl_2.2H_2O$ at 200 °C, and then, dried up at 400 °C under the flowing argon. Appropriate amounts of BaF_2 and $BaCl_2$ are homogenized and then palletized. These pellets were heated at 800 °C for 16 h in a platinum boat under argon. The temperature was raised at 5 °C/min and cooled back to room temperature at 3 °C/min. The colorless product obtained was characterized by powder x-ray and neutron diffraction for its phase purity.

The phonon density of states are measured using[23] a medium-resolution triple-axis spectrometer at Dhruva reactor at Trombay. About 40 g of a BaFCl polycrystalline sample is placed in a thin aluminum container for neutron measurements. Neutrons of a fixed final energy E_f are observed using a pyrolytic graphite (002) analyzer, while the incident energy is varied using a copper (111) monochromator. All the mea-

TABLE I. The transferable interatomic potential parameters used in the shell model calculations.

	Ba	Sr	Pb	F	Cl	Br	I
Z	2.0	2.0	2.0	−1.0	−1.0	−1.0	−1.0
Y	3.0	3.0	4.0	−1.0	−1.0	−1.0	−1.0
K (eV/Å^2)	90	90	40	140	140	140	140
R (Å)	2.42	2.23	2.40	1.40	2.28	2.34	2.55

surements are carried out in the energy loss mode with constant momentum transfer (Q). The elastic energy resolution is about 15 % of the final energy. Several scans are recorded with E_f value of 30 meV and Q values ranging from 5 to 6 Å^{-1}. The neutron-weighted phonon density of states are obtained[24] from the measured scattering function $S(Q,E)$ via

$$g^{(n)}(E)=A\left\langle \frac{e^{2W(Q)}}{Q^2}\frac{E}{n(E,T)+1}S(Q,E)\right\rangle \tag{1}$$

$$\simeq B\sum_p \frac{4\pi b_p^2}{M_p}g_p(E), \tag{2}$$

where $n(E,T)=[\exp(E/k_BT)-1]^{-1}$.

TABLE II. Comparison between the experimental (Ref. 4) (at 293 K) and calculated structural parameters (at 0 K). For the space group $P4/nmm$, the F atoms are located at (0, 0, 0) and (0.5, 0.5, 0), the X atoms at (0, 0.5, u) and (0.5, 0, $\overline{u}$), and the M atoms at (0, 0.5, v) and (0.5, 0, $\overline{v}$).

		Experimental	Calculated
BaFCl	a (Å)	4.394	4.427
	c (Å)	7.225	7.126
	u	0.6472	0.660
	v	0.2049	0.191
BaFBr	a (Å)	4.508	4.479
	c (Å)	7.441	7.229
	u	0.6497	0.662
	v	0.1911	0.187
BaFI	a (Å)	4.654	4.634
	c (Å)	7.962	7.752
	u	0.6522	0.673
	v	0.1704	0.173
SrFCl	a (Å)	4.126	4.163
	c (Å)	6.958	6.827
	u	0.6489	0.664
	v	0.2015	0.189
SrFBr	a (Å)	4.218	4.212
	c (Å)	7.337	6.985
	u	0.6479	0.668
	v	0.1859	0.184
PbFCl	a (Å)	4.110	4.404
	c (Å)	7.246	7.079
	u	0.6497	0.660
	v	0.2058	0.191
PbFBr	a (Å)	4.18	4.451
	c (Å)	7.59	7.202
	u	0.65	0.664
	v	0.195	0.187

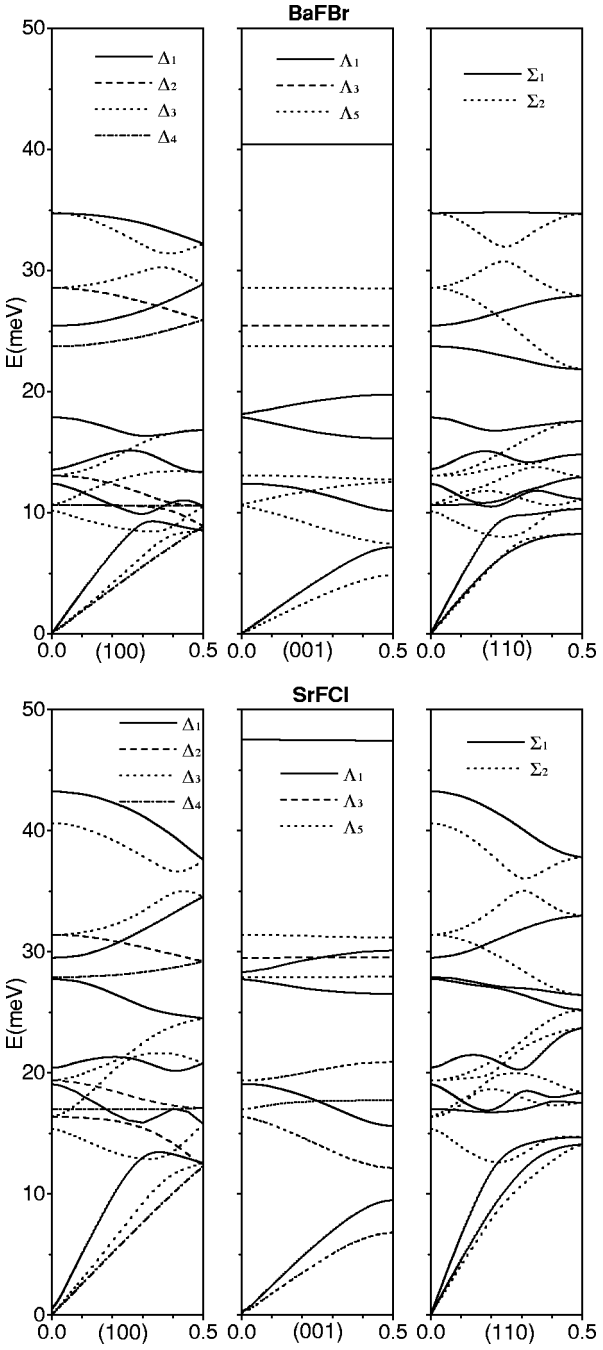

FIG. 1. The calculated phonon dispersion relation along high symmetry directions for BaFBr and SrFCl.

TABLE III. Comparison between the calculated and experimental long wavelength Raman and infrared modes in cm^{-1} units (1 cm^{-1} =0.124 meV). Experimental data: BaFCl [Refs. 14–16(a)], BaFBr [Refs. 14,17(a)] and BaFI [Ref. 16(b)], SrFCl (Refs. 14,15), PbFCl [Ref. 17(b)] and PbFBr [Ref. 17(b)].

	BaFCl			BaFBr		BaFI		SrFCl		SrFBr	PbFCl		PbFBr	
	Expt.	Expt.	Calc.	Expt.	Calc.	Expt.	Calc.	Expt.	Calc.	Calc	Expt.	Calc.	Expt.	Calc.
A_{1g}	125		123	105	100	79	78	155	154	114	105	96	89	89
	161		182	119	144	113	130	196	223	186	164	162	116	112
B_{1g}	212		207	215	205	203	199	243	238	235	226	211	224	208
E_g	89		99	76	86	70	64	107	132	97	43	79	39	76
	142		137	109	105	105	100	167	156	138	134	137	94	96
	247		239	240	230	218	210	298	253	241	240	217	224	206
A_{2u}(TO)	143		113	122	82	138	63		124	92		108		76
	293		290	299	280	270	271		327	315		285		276
A_{2u}(LO)	197	210	201	137	146		119	182	228	169		183		129
	340	294	330	330	326		315	340	383	366	340	292		287
E_u(TO)	130	113	115	98		86	77	143	137	106	125	112	78	82
	210	212	199	202	191	193	166	255	225	215	182	197	167	190
E_u(LO)	148		144	117	109	98	94		164	128		139		102
	290		296	273	280	247	255		348	319		254		245

Here A and B are normalization constants and b_p, M_p, and $g_p(E)$ are, respectively, the neutron scattering length, mass, and partial density of states of the pth atom in the unit cell. The quantity within $\langle - - - - \rangle$ represents the average over all Q values. $2W(Q)$ is the Debye-Waller factor. The factor $4\pi b_p^2/M_p$ turns out for Ba, F and Cl, atoms as 0.025, 0.211, and 0.474 barn/amu, respectively. We calculate the one phonon density of states $g(E)$ in the following way:

$$g(E)=\sum_p g_p(E). \tag{3}$$

III. LATTICE DYNAMICAL CALCULATIONS

The compounds MFX (M=Ba, Sr, Pb; X=Cl, Br, I), known as the matlockite structure compounds (space group $P4/nmm$) crystallize in the tetragonal structure, consisting of two formula units per unit cell,[4] and are formed by alternative sheets of MF_2 and MX_2. The MF_2 sublattice is made up of corner shared cation tetrahedra around a fluorine, while MX_2, of edge-shared cation pyramids inside which the atom X has an asymmetric coordination. The atom X is equidistant from the four basal -plane atoms M but at a different distance from the apex atom M.

The present lattice dynamical calculations are carried out using a shell model.[25] Each ion consists of a core and a massless shell of charge, which are connected by a harmonic spring constant. The shell can displace itself from the core causing a dipole, leading to a proper description of the crystal dielectric behavior. The following two-body potential[26] consisting of Coulombic and short-ranged Born-Mayer terms is used for describing the interactions between the ions:

$$V(r)=\frac{e^2}{4\pi\epsilon_0}\frac{Z(k)Z(k')}{r}+a\exp\left[\frac{-br}{R(k)+R(k')}\right]-\frac{C}{r^6}, \tag{4}$$

where r is the separation between the atoms of type k and k'. $R(k)$ and $Z(k)$ are the effective radius and charge of the kth atom type. a=1822 eV and b=12.364 are treated as constants. This set of parameters has been successfully used by us in the lattice dynamical calculations of several complex solids.[26,27] The van der Waals interaction (last term) in Eq. (4) is applied only between the X-M, F-F, F-X, and X-X pairs. The value of C is chosen as 90 eVÅ^6. Initially, we determine the parameters of the potential for BaFCl such that it reproduces the structure of BaFCl close to that determined by the diffraction experiments at zero pressure and also, satisfies the condition of dynamical equilibrium. For calculations of BaFBr, BaFI, SrFCl SrFBr, PbFCl, and PbFBr we have used appropriate radii parameters of Br, I, Sr, and Pb. The empirical parameters including the shell charge (Y) and shell-core force constants (K) for the ions used in the calculations are given in Table I. The calculations have been carried out using the current version of the software DISPR (Ref. 28) developed at Trombay. The calculated lattice constants and fractional coordinates of the atoms (Table II) for all the four compounds are in good agreement with experimental data.[4]

IV. RESULTS AND DISCUSSION

A. Phonon dispersion relation, Raman and infrared active modes, elastic constants, and force constants

Corresponding to the six atoms in the primitive cell, there are 18 phonon modes at every wave vector. A group theoretical analysis of the phonon dispersion relation for BaFCl at the Γ point, and along the Δ, Λ, and Σ directions, has been carried out using standard techniques.[25(b),29] The symmetry decomposition of phonon branches is given as

TABLE IV. (a) Comparison between the experimental (Ref. 11) and calculated elastic constants C_{ij} in GPa units. The experimental data under [a] and [b] are measured using ultrasonic and Brillouin scattering techniques respectively. The experimental (Ref. 11) errors reported are up to 2.5 GPa except in C_{12} and C_{13} for BaFBr, BaFI, SrFCl, and SrFBr, where these are up to 7.7 GPa. (b) Comparison between the experimental and calculated bulk modulus B(GPa) and its pressure derivative B'. The experimental data under [a], [b] and [c] are from Refs. 11, 4,5(a), and 6, respectively. The data under [a] have been obtained using elastic constants, and the data under [b] and [c] from the Murnaghan equation of state (Ref. 34). The calculated bulk modulus [d] using the TB-LMTO method is from Ref. 19.

(a)

	Elastic constant	Experimental		Calculated
		[a]	[b]	
BaFCl	C_{11}	71.9	75.9	84.9
	C_{33}	65.6	65.9	58.8
	C_{44}	20.4		26.2
	C_{66}	23.8		26.2
	C_{12}	28.2		32.6
	C_{13}	31.9		34.5
BaFBr	C_{11}		71.3	79.7
	C_{33}		55.4	53.5
	C_{44}		20.9	25.1
	C_{66}		24.7	22.7
	C_{12}		25.0	29.1
	C_{13}		34.3	32.1
BaFI	C_{11}		55.8	63.7
	C_{33}		31.9	31.1
	C_{44}		19.2	20.3
	C_{66}		24.3	22.9
	C_{12}			23.8
	C_{13}		23.5	23.8
SrFCl	C_{11}	93.8	91.2	107.3
	C_{33}	76.8	77.0	65.7
	C_{44}	28.7	29.5	34.6
	C_{66}	31.5	30.9	26.8
	C_{12}	29.6	29.0	38.2
	C_{13}		40.2	42.4
SrFBr	C_{11}		88.7	100.3
	C_{33}		53.3	54.7
	C_{44}		27.4	32.4
	C_{66}			27.0
	C_{12}			35.6
	C_{13}		35.3	38.5
PbFCl	C_{11}			86.0
	C_{33}			60.2
	C_{44}			26.8
	C_{66}			22.7
	C_{12}			17.6
	C_{13}			35.3
PbFBr	C_{11}			81.4
	C_{33}			53.1
	C_{44}			25.7
	C_{66}			23.1
	C_{12}			19.3
	C_{13}			32.7

TABLE IV. (*Continued*).

(b)

	Experimental					Calculated		
	[a]	[b]	[b]	[c]	[c]	This work		[d]
	B	B	B'	B	B'	B	B'	B
BaFCl	44.4	45±3	5.2±0.5	62±6	4±1	46	4.2	62
BaFBr	42.6	42±6	6±2	44±7	5±1	43	4.2	44
BaFI		36±5	6±1			34	4.3	41
SrFCl	53.7			61±4	5±1	55	4.3	61
SrFBr		51±10	6±2			49	4.9	
PbFCl						47	4.1	
PbFBr		43±15	6±3			44	4.2	

$$\Gamma: 2A_{1g}+3A_{2u}+B_{1g}+3E_g+3E_u,$$

$$\Delta = 6\Delta_1+3\Delta_2+6\Delta_3+3\Delta_4,$$

$$\Lambda = 5\Lambda_1+\Lambda_3+12\Lambda_5,$$

$$\Sigma = 9\Sigma_1+9\Sigma_2.$$

The A_{1g}, B_{1g}, and E_g modes are Raman active while the A_{2u} and E_u modes are infrared active. A group theoretical analysis has been useful to block diagonalize the dynamical matrices in lattice dynamical calculations, and also to distinguish various phonon branches in different group theoretical representations. There are 18 distinct dispersion branches along [100] and [110] direction, while along [001] the number of distinct branches are 12 due to the degeneracy of phonons in Λ_5.

We have shown typical phonon dispersion relations in Fig. 1 for BaFBr and SrFCl. The calculated dispersion relations for BaFBr show that there is a gap around 20 meV, which is also observed in the phonon density of states shown below. Some of the phonon dispersion branches in the three directions at the Brillouin zone center do not agree because of LO-TO splitting of phonons. Table III shows the comparison between our calculated long wavelength Raman and infrared modes with the experimental data.[14–17] The average deviation of our calculations from the experimental optical data is about 6%, 9%, 10%, 12%, 16%, and 17% for BaFCl, BaFBr, BaFI, SrFCl, PbFCl, and PbFBr, respectively (Table III). Two experimental data sets[15,16] are available in the literature for the infrared phonons in BaFCl, which show differences of about 10%. In case of BaFI, a large discrepancy is observed for the A_{2u}(TO) mode. This mode is reported at nearly the same frequency in both the BaFBr and BaFI in experiments. However, as may be expected from mass consideration, the calculated value of this mode for BaFI is the lowest among BaX compounds. In the case of Pb compounds our calculations do not reproduce the lowest E_g mode frequency very satisfactorily, although for other modes the agreement is good. No experimental data are available for SrFBr. The large LO-TO splitting (Table III) for the A_{2u} and E_u modes has been fairly well described by our calculation.

The calculated elastic constants (obtained from the slopes of the acoustic phonon branches near the zone center) and bulk modulii are also found to be in good agreement with the available experimental data[11] as displayed in Table IV. The experimental data of elastic constants are not available for PbFCl and PbFBr, and so the predictions alone are given in Table IV. The ratio C_{33}/C_{11} gives an idea of the nature of forces between the interlayer and intralyer bonds[11] in the layered compounds. For BaX (X=Cl, Br, I) compounds this calculated ratio varies from 0.7 for BaFCl to 0.5 for BaFI, which indicates that for BaFI the interlayer bonds are weaker in comparison of intralayer bonds. This may be expected since the structure becomes less compact as the size of X ion increases from Cl to I. On the other hand for MFCl (M=Ba, Sr, Pb) this calculated ratio shows a small variation from 0.70 for PbFCl to 0.6 for SrFCl, perhaps since the nature of interlayer forces is mainly determined by the X ions.

In Table V, we have given the calculated transverse and longitudinal force constants for the first neighbors of the metal ion. The force constants for the M-F bonds are larger than those for the M-X bonds which reflect their relative strengths.

TABLE V. The calculated longitudinal (∂^2V/∂^2r) and transverse force constants ($1/r\,\partial V/\partial r$) for the first neighbors of metal ions in units of eV/Å^2.

	$\frac{\partial^2V}{\partial^2r}$		$\frac{1}{r}\frac{\partial V}{\partial r}$	
	M-F	M-X	M-F	M-X
BaFCl	0.96	0.25	1.14	0.59
BaFBr	0.79	0.28	1.13	0.57
BaFI	0.30	0.39	1.12	0.48
SrFCl	1.14	0.37	1.36	0.70
SrFBr	0.92	0.41	1.35	0.67
PbFCl	0.97	0.25	1.16	0.60
PbFBr	0.80	0.29	1.16	0.57

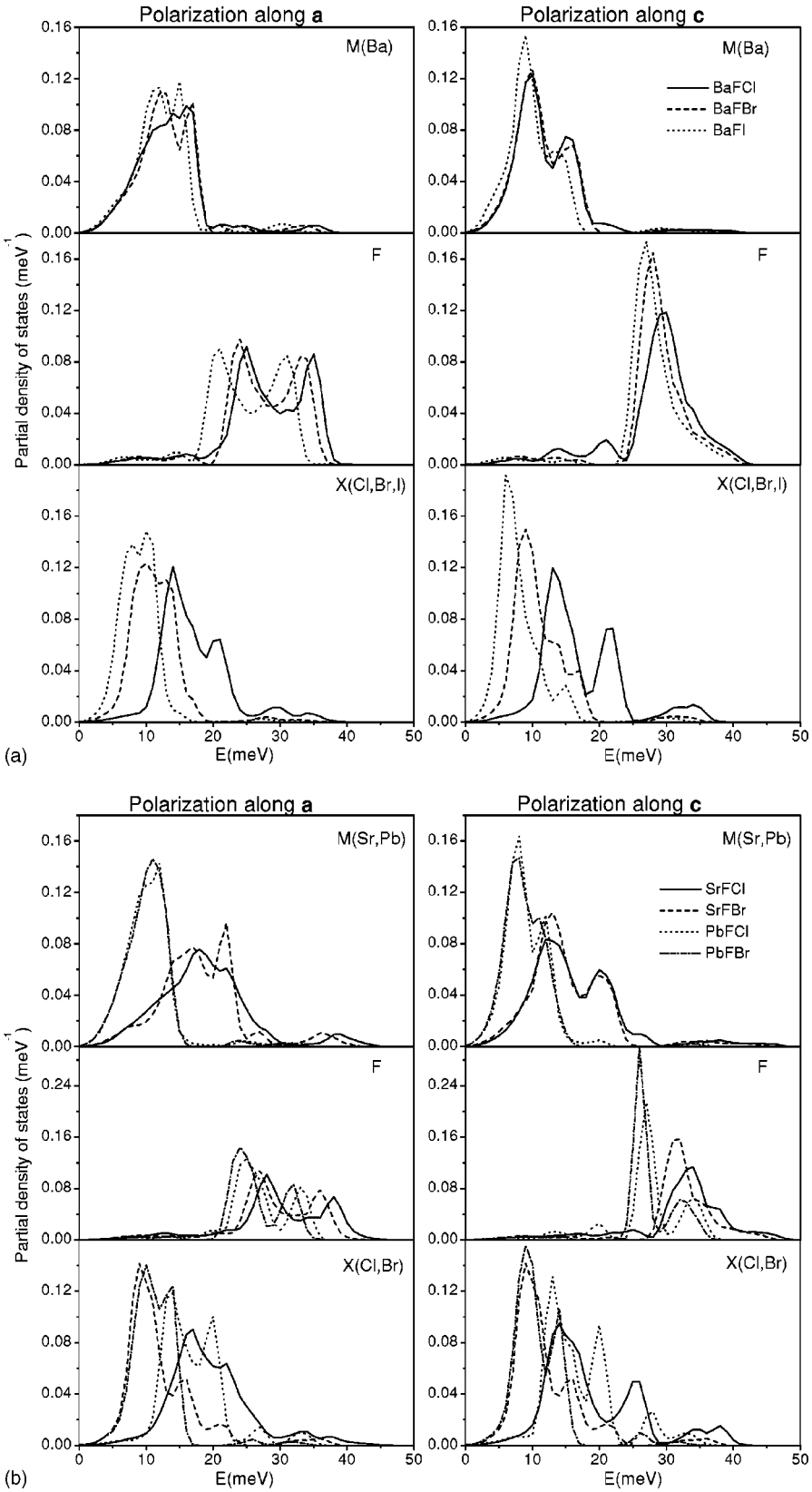

FIG. 2. The calculated partial density of states for various atoms in (a) BaFCl, BaFBr, and BaFI and (b) SrFCl, SrFBr, PbFCl, and PbFBr. The contributions from the polarization along the a and c directions are shown in the left and right columns. The contributions are identical along the a and b directions due to the tetragonal symmetry.

B. Partial density of states and anisotropic thermal parameters

The dynamical contributions to frequency distribution arising from the various species of atoms can be observed from their partial densities of states, which are obtained[30] by atomic projections of the one-phonon eigenvectors. Contributions from 288 wave vectors in the irreducible Brillouin zone have been used for obtaining the phonon spectrum. The calculated partial density of states for various atoms are shown in Fig. 2. The Ba atoms contribute largely up to 20

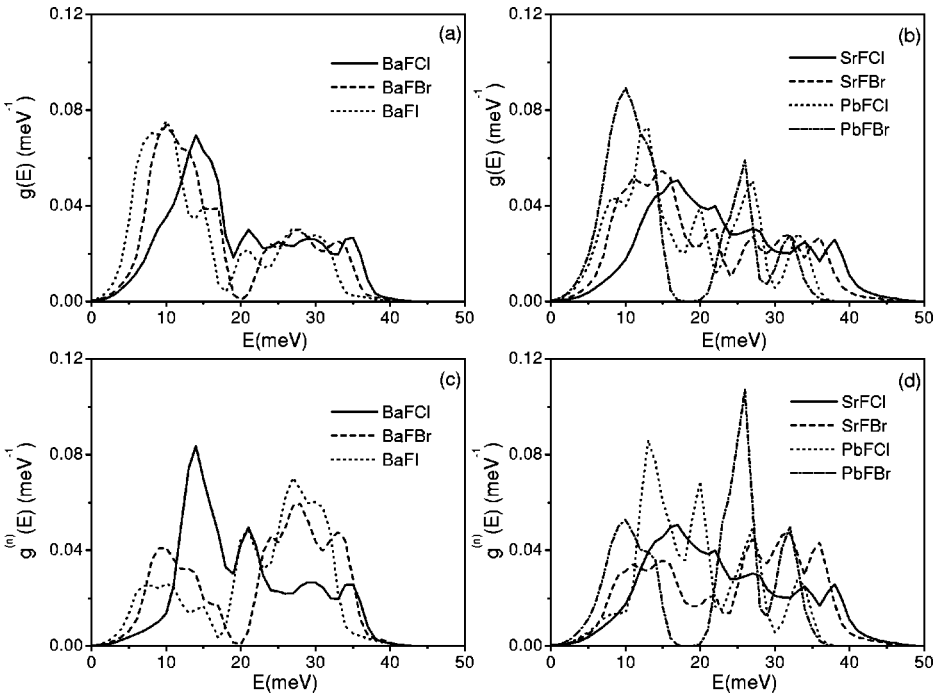

FIG. 3. The calculated phonon density of states $g(E)$ and neutron-weighted phonon density of states $g^{(n)}(E)$. The calculated spectra have been convoluted with a Gaussian with a full width at half maximum (FWHM) of 2 meV.

meV, while the contributions from Sr and Pb atoms are up to 25 and 15 meV, respectively. Such a variation is partly expected due to the mass effect. The contributions due to F atoms in all the compounds occurs above 20 meV. There are two peaks in the partial density of states for the F atoms for the polarization along the a direction, while along *c* direction there is only one peak, which shows the anisotropy of the in-plane and out-of-plane vibrations. The F vibrations are extended up to 40, 45, and 37 meV in Ba, Sr, and Pb compounds, respectively. The vibrations due to Cl atoms are up to 25, 30, and 25 meV in BaFCl, SrFCl, and PbFCl, respectively, while for Br atoms the corresponding range is 20, 25, and 17 meV in BaFBr, SrFBr, and PbFBr, respectively (Fig. 2). The I vibrations in BaFI extends upto 17 meV. In general, the energy range of vibrations due to different atoms in Sr compounds is more than that in Ba and Pb compounds.

The calculated total density of states in Figs. 3(a) and 3(b) show that, for Ba, Sr, and Pb compounds, the range of the phonon spectra extend up to about 40, 45, and 37 meV, respectively. In the case of BaFBr and PbFBr, we observe a gap in the phonon spectrum at about 20 meV (Figs. 1 and 3). This gap arises since the vibrations due to both the M(Ba, Pb) and Br atoms occur below 20 meV, largely due to their heavier masses, and the vibrations of F atoms occur above 20 meV. The calculated partial phonon density of states (Fig. 2) clearly indicate that the phonon spectra [Figs. 3(a) and 3(b)] of these compounds are highly sensitive to substitution of the M(Ba, Sr, Pb) or X(Cl, Br, I) atoms.

The partial density of states have been used for the calculation of the anisotropic thermal parameters at different temperatures. A comparison between the calculated and experimental values for BaFCl is given in Table VI. The experimental values of U_{11} for Cl in BaFCl is about 10% more than that of U_{33}, which is in contrast to the trend observed for Ba and F. However, our calculation shows that, also for Cl, U_{33} is more than U_{11}. However, the anisotropy is not significant for BaFCl. The overall good agreement between the experiment and calculations reflect the reliability of the calculated partial density of states. Since the experimental data of anisotropic thermal parameters are not available for BaFBr, BaFI, SrFCl, SrFBr, PbFCl, and PbFBr, we give only the predicted values in Table VII. The difference in the calculated values of U_{11} and U_{33} for different atoms shows the anisotropy of vibrations along [100] and [001]

TABLE VI. Comparison between experimental (Ref. 7) and calculated anisotropic thermal parameters (10^{-4} Å^2) of BaFCl.

	Experimental						Calculated					
	Ba		F		Cl		Ba		F		Cl	
T (K)	U_{11}	U_{33}	U_{11}	U_{33}	U_{11}	U_{33}	U_{11}	U_{33}	U_{11}	U_{33}	U_{11}	U_{33}
100							29	36	59	60	60	65
297	86(3)	99(5)	125(4)	132(6)	159(2)	137(3)	79	98	129	131	151	164
562	182(1)	217(2)	243(14)	260(24)	306(7)	284(11)	149	184	234	238	280	305
883	333(4)	385(4)	486(28)	473(45)	555(15)	499(23)	233	288	364	371	438	478

TABLE VII. The calculated anisotropic thermal parameters (10^{-4} Å^2) for BaFBr, BaFI, SrFCl, SrFBr, PbFCl, and PbFBr.

		M(Ba,Sr,Pb)		F		X(Cl,Br,I)	
	T (K)	U_{11}	U_{33}	U_{11}	U_{33}	U_{11}	U_{33}
BaFBr	100	30	37	61	61	54	61
	297	80	102	134	135	149	168
	562	151	192	243	245	279	315
	883	236	301	379	381	437	494
BaFI	100	34	49	72	71	55	71
	297	93	138	165	162	154	202
	562	175	261	302	298	290	381
	883	274	409	472	464	456	599
SrFCl	100	26	34	54	52	49	57
	297	66	89	113	110	118	143
	562	123	166	204	199	218	265
	883	192	260	316	308	341	414
SrFBr	100	28	38	57	56	45	56
	297	71	102	121	120	120	153
	562	133	190	220	217	224	288
	883	208	298	342	337	352	452
PbFCl	100	29	36	63	63	61	65
	297	82	101	138	136	152	165
	562	154	189	252	251	283	307
	883	242	297	393	391	443	481
PbFBr	100	30	37	65	64	55	62
	297	83	105	144	141	150	170
	562	156	198	264	257	281	319
	883	245	311	411	401	440	501

direction. Since the interatomic forces in these layered compounds are stronger in the ab plane and weaker along the c direction, U_{11} is in general expected to be smaller than U_{33}.

C. Neutron inelastic scattering and phonon density of states

The experimental data on BaFCl obtained for different momentum transfers Q have been averaged to obtain the neutron-weighted phonon density of states $g^{(n)}(E)$ (Fig. 4). The multiphonon scattering is estimated using the Sjolander formalism.[31] Multiple scattering is estimated at about 1%, and therefore its effect on the results has been neglected. The experimental neutron weighted phonon density of states $g^{(n)}(E)$ for BaFCl consist of phonon bands centered at about 16 and 32 meV.

The calculated $g^{(n)}(E)$ for BaFCl (Fig. 4), as obtained from the partial density of states using Eq. (2), reproduces all the main features of the experimental data. We have also calculated similar spectra [Figs. 3(c) and 3(d)] for BaFBr, BaFI, SrFCl, SrFBr, PbFCl, and PbFBr. $g^{(n)}(E)$ for BaFBr and PbFBr shows that there are two well separated bands centered around 10 and 30 meV. For other compounds also there are two phonon bands with nearly similar energy, but the bands are not well-separated as in BaFBr and PbFBr. The neutron spectra for the Ba, Sr, and Pb compounds extend up to 40, 45, and 37 meV, respectively.

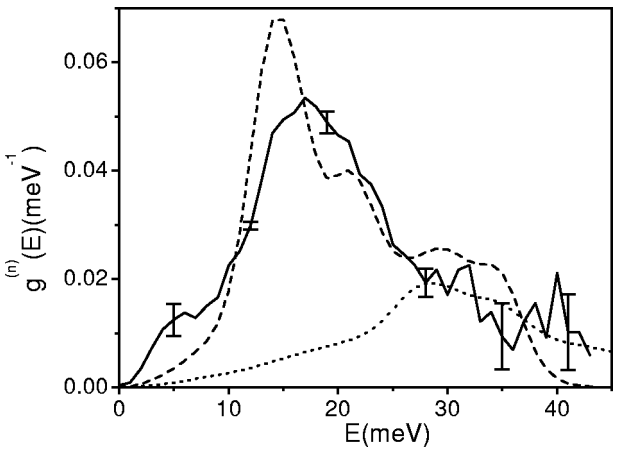

FIG. 4. The experimental (solid line) and calculated (dash line) neutron-weighted phonon density of states in BaFCl. The multiphonon contribution (dotted line) has been subtracted from the experimental data to obtain the experimental one-phonon spectrum. The calculated spectra have been convoluted with a Gaussian with a FWHM of 4 meV in order to correspond to the energy resolution in the experiment.

D. Thermodynamic properties: specific heat, thermal expansion, and equation of state

The specific heat $C_P(T)$ is derived (Fig. 5) using the calculated phonon density of states [Figs. 3(a) and 3(b)] together with the relation C_P-$C_V = \alpha_V^2 BVT$, where α_V is the volume thermal expansion (shown below) and B is the bulk modulus. There is a large variation in the measured specific heat[12,13] of all these compounds at low temperature [Figs. 5(a) and 5(b)]. The agreement between the experimental data and calculations is very good for Ba and Sr compounds [Figs. 5(a) and 5(b)]. However for Pb compounds there is an apparent discrepancy [Fig. 5(b)] between our calculations and experimental data. The low temperature specific heat below 40 K is mainly determined by the acoustic phonon modes. The only other available experimental data representing the acoustic phonons is the bulk modulus (of PbFBr), and that is well reproduced by the present model calculations (as shown below). It should also be noted that the reported experimental specific heat[13(b)] (per mole) for PbFCl is more than that of PbFBr, which may not be expected due to mass effect, and is in contrast to the calcualtion. The calculated specific heat upto 900 K is shown in Figs. 5(c) and 5(d). The C_P-C_V values range from 11% (SrFCl) to 20% (BaFI) at the highest temperature of 900 K. We have also calculated the Debye temperature of these compounds using the methods given in Ref. 25. The calculated Debye temperature [Figs. 5(e) and 5(f)] particularly in the low temperature region below 40 K, varies from 244 to 260, 203 to 234, 164 to 197, 302 to 337, 238 to 266, 203 to 236 and 181 to 204 for BaFCl, BaFBr, BaFI, SrFCl, SrFBr, PbFCl, and PbFBr, respectively, which is in good agreement with the experimental average values[12,13] of 249, 217, 188, 305, 260, 204, and 177 K, respectively from low temperature C_P measurements up

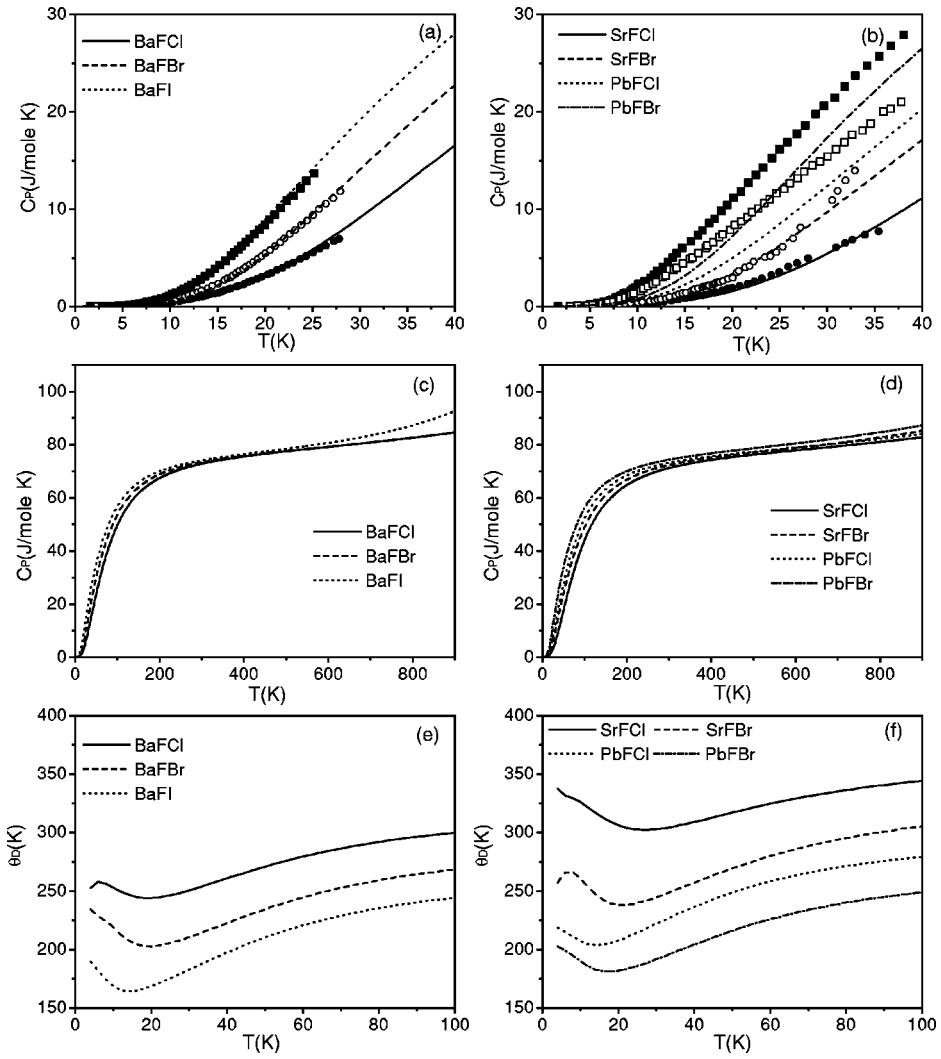

FIG. 5. The comparison between the calculated and experimental low temperature specific heat data. Experimental data: (a) BaFCl (Ref. 12) (solid circle), BaFBr (Ref. 12) (open circle), BaFI (Ref. 12) (solid squares). (b) SrFCl [Ref. 13(a)] (solid circle), SrFBr [Ref. 13(a)] (open circle), PbFCl [Ref. 13(b)] (solid squares), and PbFBr [Ref. 13(b)] (open squares). The reason for the discrepancy in the specific heat of Pb compounds is discussed in the text. (c) and (d) The calculated specific heat up to 900 K. (e) and (f) The variation of Debye temperature with temperature as obtained from lattice dynamical calculations.

to 40 K. The calculated values of Debye temperature at 900 K for BaFCl, BaFBr, BaFI, SrFCl, SrFBr, PbFCl, and PbFBr are 318, 290, 264, 364, 329, 296, and 268 K, respectively. The excellent agreement between the measured and the calculated C_P and Debye temperature at low temperatures, provides further support for the present lattice dynamical model.

In the quasiharmonic approximation each phonon mode of energy E_i contributes $(1/BV)\Gamma_i C_{Vi}$ to the thermal expansion[25–27] (where Γ_i is the mode Grüneisen parameter, V is the unit cell volume, B is the bulk modulus, C_{Vi} is the contribution of the phonon mode of energy E_i to the specific heat). This procedure is applicable when explicit anharmonicity of phonons (due to thermal amplitudes) is not very significant, and the thermal expansion arises mainly from the implicit anharmonicty, due to the change of phonon frequencies with volume. We have also included the contribution to thermal expansion arising from variation of bulk modulus with volume.[32,33] The Grüneisen parameter $(\Gamma = -\partial \ln E/\partial \ln V)$ averaged over the whole Brillouin zone as a function of phonon energy (E), is calculated [Figs. 6(a) and 6(b)] by taking the contributions of 288 wave vectors in the irreducible Brillouin zone. The values of $\Gamma(E)$ averaged over phonon energies are 1.57, 1.49, 1.34, 1.42, 1.38, 1.47 and 1.59 for BaFCl, BaFBr, BaFI, SrFCl, SrFBr, PbFCl, and PbFBr, respectively. The Γ values lie between 1.0 and 2.5 for phonons of energies up to about 25 meV, and Γ decreases above 25 meV. In case of BaFI for low energy modes about 5 meV, Γ lies between 2.5 and 3.5. The calculated thermal expansion [Fig. 6(c)] for BaFCl is in good agreement with the experimental data available from Refs. 7 and 8. The predication of volume thermal expansion is also given for the remaining compounds in Figs. 6(c) and 6(d). For BaFI and PbFBr thermal expansion is large in comparison with the remaining five compounds. The thermal expansion coefficient is nearly the same for BaFCl, BaFBr, SrFBr, and PbFCl, while it is the least for SrFCl.

In order to understand the contribution of various phonons to the thermal expansion coefficient α_V at a particular temperature, we have calculated the contribution from phonons of various energies to the total thermal expansion at 500 K [Figs. 6(e) and 6(f)]. The maximum contribution to α_V in BaFCl, BaFBr, and BaFI is from phonons of energies around 15, 10, and 7 meV, respectively. In SrFCl and SrFBr the contribution from phonons of energy 10-25 and 8–17 meV, respectively, is at a maximum. In addition to low energy phonons higher energy phonons also contribute significantly

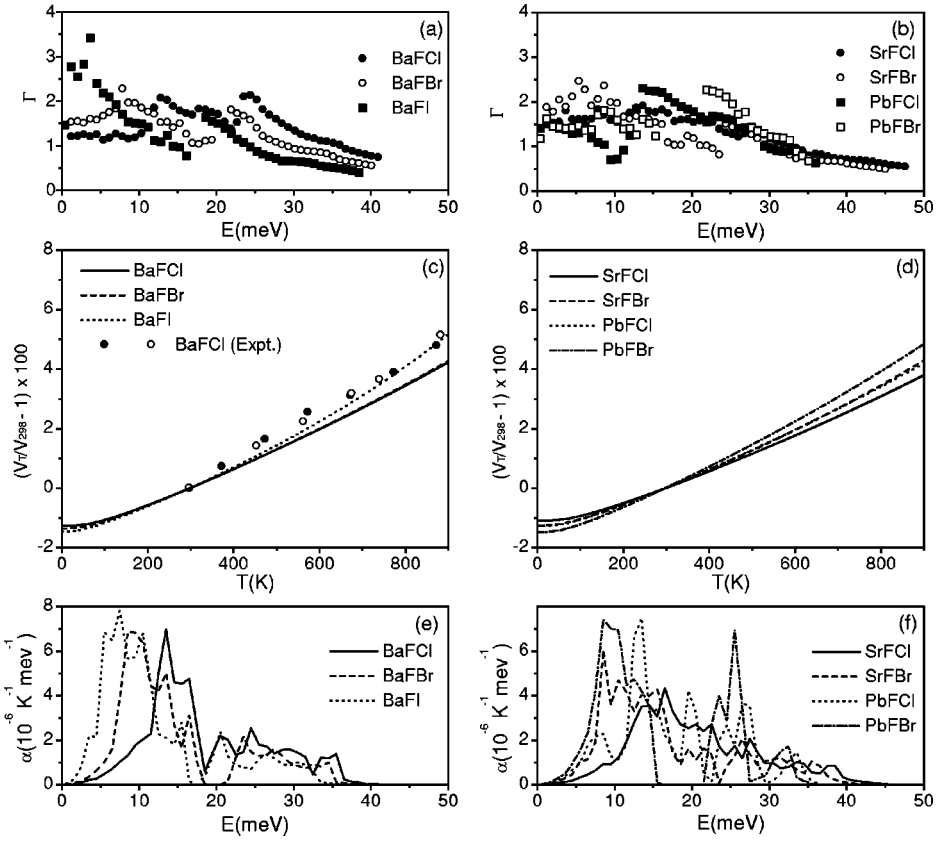

FIG. 6. (a) and (b) The calculated mode Grüneisen parameter $\Gamma(E)$ averaged for phonons of energy E. (c) Comparison between the calculated (solid line) and experimental data (symbols) of unit cell volumes (Refs. 7 and 8) at different temperatures for BaFCl. The open and solid circles corresponds to experimental data for BaFCl from Refs. 7 and 8 respectively. The calculated thermal expansion behavior for BaFBr and BaFI is also shown. (d) The calculated thermal expansion behavior for SrFCl, SrFBr, PbFCl, and PbFBr, $(V_T/V_{298}-1)\times 100\%$, V_T and V_{298} being the cell volumes at temperatures T and 298 K, respectively. (e) and (f) The contribution of phonons of energy E to the volume thermal expansion as a function of E at 500 K.

to α_V in PbFCl and PbFBr. The calculated partial density of states (Fig. 2) show that in Ba and Sr compounds the phonons which contribute to α_V are mainly M(Ba,Sr) and X(Cl, Br, I) atoms. The contribution to α_V due to F atoms occurs from phonons above 20 meV, is less significant in Ba and Sr compounds, and is relatively more significant in Pb compounds.

The high-pressure response of the unit cell parameters has been measured[4,5(a),6] using x-ray diffraction. The experimental data for BaFCl and BaFBr are available up to 28 GPa. There is a crystal to crystal phase transition at pressures above 21 and 27 GPa for BaFCl and BaFBr, respectively. For BaFI Raman scattering experiments[5(b)] show a crystal to crystal phase transition at 55 GPa, while x-ray diffraction data[4] are available only up to 35 GPa. SrFCl, SrFBr, and PbFBr show no phase transition[5(a),6] upto 42, 30, and 30 GPa, respectively, while for PbFCl no high-pressure x-ray diffraction data are available. The experiments for BaFCl, BaFBr, and BaFI were reported[4] using argon and silicon oil pressure transmitting media. The data for SrFCl are obtained[6] with ethanol, methanol and water mixture, while in case of SrFBr and PbFBr data[5(a)] with only silicon oil are reported. However, due to the glass transition of the silicon oil above 10 GPa, a strong and gradual broadening of the diffraction lines from the samples (BaFCl, BaFBr, BaFI, SrFBr, and PbFBr) was observed.[4,5(a)] The crystal structures for these compounds at different pressures are calculated by minimization of the free energy in our calculations. The anisotropic behavior of the compression of unit cell parameters along a and c directions is fairly well reproduced. The calculated equation of state (Fig. 7) is in good agreement with the experimental data[4] for BaFCl, BaFBr, BaFI, and SrFCl. There is a slight disparity between the calculated and experimental data in SrFBr and PbFBr above 10 GPa due to problems associated with pressure transmitting medium as noted above. Our prediction of the equation of state for PbFCl is also given in the same figure.

The bulk modulus and its pressure derivative for all the four compounds have been determined [Table IV(b)] by fitting the calculated volume data at different pressures to the Murnaghan equation of state.[34] The same value of bulk modulus is also derived from the calculated elastic constants. Kalpana *et al.*[19] estimated the bulk modulus for these compounds from the tight-binding linear muffin-tin orbital (TB-LMTO) method within the local density approximation (LDA).[35] Table IV(b) provides a comparison between the various experiments and calculations of the bulk modulus. The present calculations compare very well the experimental data. Our calculations show that there is a large variation in the calculated values of Bulk modulus for these compounds, which varies from 34 GPa (BaFI) to 55 GPa (SrFCl). The experimental data also show a similar behavior (Table IV).

V. CONCLUSIONS

We have developed a lattice dynamical model for BaFCl and validated it by numerous experimental data including our phonon density of states measurements from polycrystalline sample of BaFCl. The model is then transferred to

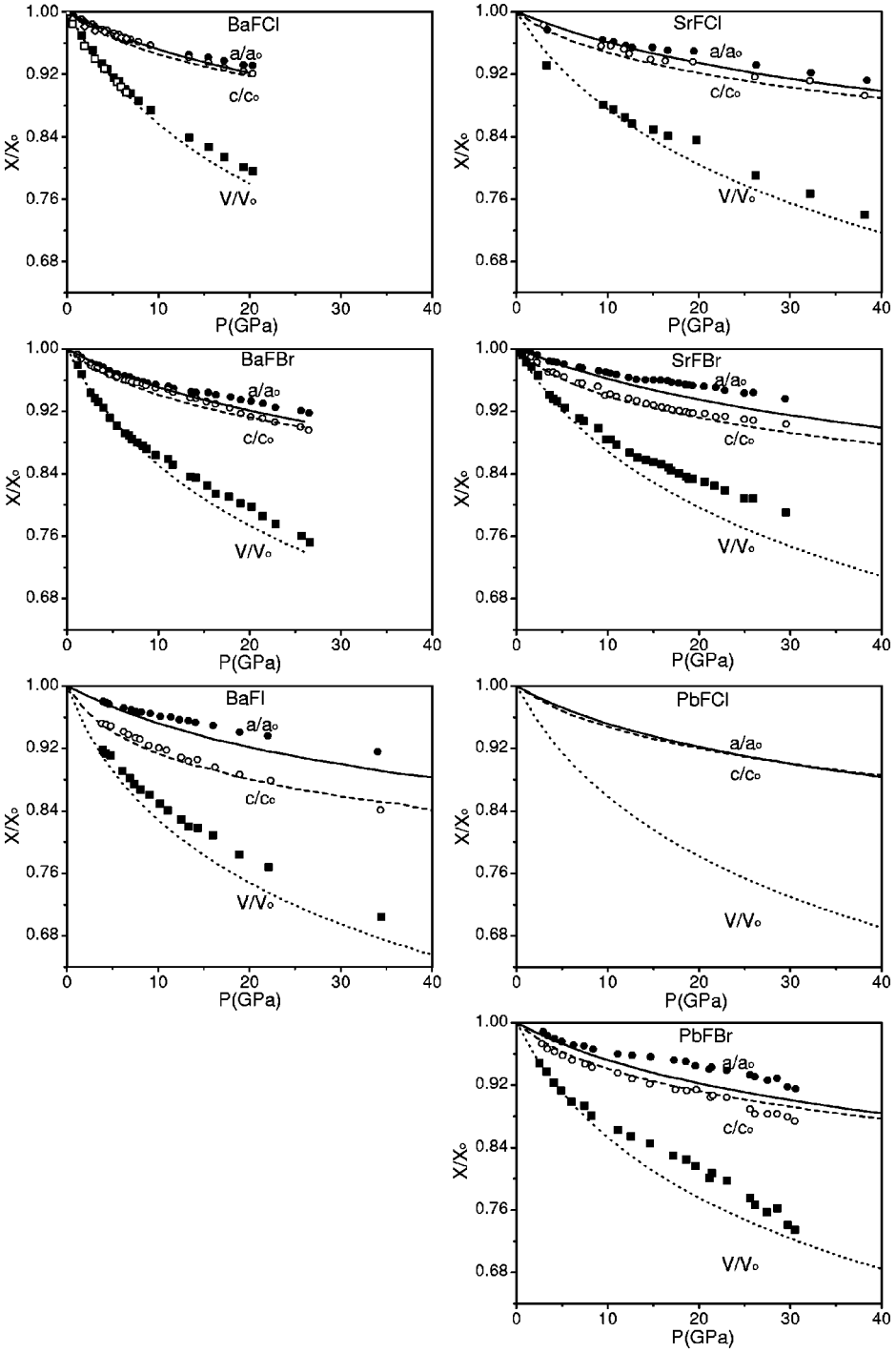

FIG. 7. Comparison between the calculated and experimental equations of state for BaFCl, BaFBr, BaFI, SrFCl, SrFBr, and PbFBr. The experimental data of equation of state for PbFCl are not available. The solid circles, open circles and solid squares are the experimental data respectively for a/a_o, c/c_o, and V/V_o. The solid lines, dashed lines, and dotted lines correspond to calculated a/a_o, c/c_o, and V/V_o. The experimental data for BaFCl, BaFBr, BaFI, SrFCl, SrFBr, and PbFBr are from Refs. 4,4,4,6,5(a),5(a), respectively. Another set of experimental data [Ref. 3(b)] for BaFCl for a/a_o, c/c_o, and V/V_o are shown by the solid diamond, open diamond and open squares, respectively. $X_o(a_o, c_o, V_o)$ and $X(a,c,V)$ refer to the values at ambient pressure and pressure P, respectively. The reason for large discrepancy in the equation of state data for SrFBr and PbFBr above 10 GPa is explained in the text.

BaFBr, BaFI, SrFCl, SrFBr, PbFCl, and PbFBr by changing only the potential parameter associated with the radii of Sr, Pb, Br and I atoms. The differences in the calculated phonon spectra in these compounds arise from both mass and potential variations, and are shown to manifest in the thermodynamic properties of these compounds. In particular, the large differences in the observed specific heat in the Ba and Sr compounds are beautifully reproduced in our calculations. The lattice dynamical calculations also enabled us to understand contributions from various phonons to the total thermal expansion. We have made it possible to provide predictions on the thermal expansion and the equation of state wherever experimental data are not yet available. Further, our studies have enabled a microscopic interpretation of the available experimental data and have been useful in the calculation for various thermodynamic properties at high pressure and temperature of these compounds.

ACKNOWLEDGMENTS

A.S. expresses his deep sense of gratitude to the Council of Scientific & Industrial Research (CSIR), India, for rendering necessary financial assistance during the work.

[1] G. J. Piermarini, S. Block, and J. D. Barnett, J. Appl. Phys. **44**, 5377 (1973).
[2] Y. R. Shen, T. Gregorian, and W. B. Holzapel, High Press. Res. **7**, 73 (1991).
[3] (a) N. Subramanian, N. V. Chandra Shekhar, P. Ch. Sahu, Mohammad Yousuf, and K. Govinda Rajan, Phys. Rev. B **58**, R555 (1998). (b) H. P. Beck and A. Limmer, Acta Crystallogr. Sect. B Struct. Sci. **39**, 401 (1983).
[4] F. Decremps, M. Fischer, A. Polian, and J. P. Itie, Phys. Rev. B **59**, 4011 (1999).
[5] (a) F. Decremps, M. Fischer, A. Polian, J. P. Itie, and M. Sieskind, Eur. Phys. J. B **9**, 49 (1999). (b) F. Decremps, M. Gauthier, J.-C. Chervin, M. Fischer, and A. Polian, Phys. Rev. B **66**, 024115 (2002).
[6] Y. R. Shen, U. Englisch, L. Chudinovskikh, F. Porsch, R. Haberkorn, H. P. Beck, and W. B. Holzapfel, J. Phys.: Condens. Matter **6**, 3197 (1994).
[7] N. Kodama, K. Tanaka, T. Utsunomiya, Y. Hoshino, and F. Marumo, Solid State Ionics **14**, 17 (1984).
[8] R. Kesavamoorthy, B. Sundarakkannan, G. V. Narasimha Rao, and V. Sanakara Sastry, Thermochim. Acta **307**, 185 (1997).
[9] T. Kurobori, Y. Hirose, and M. Takeuchi, Phys. Status Solidi B **220**, R11 (2000).
[10] F. Decremps, M. Fischer, A. Polian, and M. Sieskind, Eur. Phys. J. B **5**, 7 (1998).
[11] F. Decremps, M. Fischer, and A. Polian, High Temp.-High Press. **30**, 235 (1998).
[12] Y. Dossmann, R. Kuentzler, M. Sieskind, and D. Ayachour, Solid State Commun. **72**, 377 (1989).
[13] (a) M. Sieskind, Y. Dossmann, R. Kuentzler, and J. P. Lambour, Phys. Status Solidi A **148**, 153 (1995). (b) M. Sieskind, J. P. Lambour, Ch. Steer, and G. Guigue, *ibid.* **145**, 89 (1994).
[14] J. F. Scott, J. Chem. Phys. **49**, 2766 (1968).
[15] H. L. Bhatt, M. R. Srinivasan, S. R. Girisha, A. H. Rama Rao, and P. S. Narayanan, Indian J. Pure Appl. Phys. **15**, 74 (1977).
[16] (a) M. Sieskind, M. Ayadi, and G. Zachmann, Phys. Status Solidi B **136**, 489 (1986). (b) M. Sieskind, D. Ayachour, J.-C. Merle, and J.-C. Boulou, *ibid.* **158**, 103 (1990).
[17] (a) H. E. Rast *et al.*, J. Chem. Phys. **55**, 1484 (1971). (b) A. Rulmont, Spectrochim. Acta A **30**, 161 (1974).
[18] R. C. Baetzold, Phys. Rev. B **36**, 9182 (1987).
[19] G. Kalpana, B. Palanivel, and I. B. Shameem Banu, Phys. Rev. B **56**, 3532 (1997).
[20] K. R. Balasubramanian and T. M. Haridasan, J. Phys. Chem. Solids **42**, 667 (1981).
[21] K. R. Balasubramanian, T. M. Haridasan, and N. Krishnamurthy, Chem. Phys. Lett. **67**, 530 (1979).
[22] M. Liu, T. Kurobori, and Y. Hirose, Phys. Status Solidi B **225**, R20 (2001).
[23] S. L. Chaplot, R. Mukhopadhyay, P. R. Vijayaraghavan, A. S. Deshpande, and K. R. Rao, Pramana, J. Phys. **33**, 595 (1989).
[24] D. L. Price and K. Skold, in *Neutron Scattering*, edited by. K. Skold and D. L. Price (Academic Press, Orlando, 1986), Vol. A; J. M. Carpenter and D. L. Price, Phys. Rev. Lett. **54**, 441 (1985); S. N. Taraskin and S. R. Elliott, Phys. Rev. B **55**, 117 (1997).
[25] (a) P. Bruesch, in *Phonons: Theory and Experiments* (Springer, Berlin 1982). (b) G. Venkatraman, L. Feldkamp, and V. C. Sahni, *Dynamics of Perfect Crystals* (MIT Press, Cambridge, MA, 1975).
[26] R. Mittal and S. L. Chaplot, Phys. Rev. B **60**, 7234 (1999).
[27] R. Mittal, S. L. Chaplot, and N. Choudhury, Phys. Rev. B **64**, 094302 (2001).
[28] S. L. Chaplot (unpublished).
[29] K. R. Rao, S. L. Chaplot, V. M. Padmanabhan, and P. R. Vijayaraghavan, Pramana **19**, 593 (1982); O. V. Kovalev, *Irreducible Representations of Space Groups* (Gordon and Breach, New York, 1964); C. J. Bradely and A. P. Cracknell, *The Mathematical Theory of Symmetry in Solids* (Oxford University Press, Oxford, 1972).
[30] N. Choudhury, S. L. Chaplot, and K. R. Rao, Phys. Chem. Miner. **16**, 599 (1989).
[31] A. Sjolander, Ark. Fys. **14**, 315 (1958).
[32] V. K. Jindal and J. Kalus, Phys. Status Solidi B **133**, 89 (1986).
[33] R. Bhandari and V. K. Jindal, J. Phys.: Condens. Matter **3**, 899 (1991).
[34] F. Birch, J. Geophys. Res. **57**, 227 (1952).
[35] K. Andersen and O. Jepsen, Phys. Rev. Lett. **53**, 2571 (1984).